A Subband Coding, BCH Coding, and 16-QAM System for Mobile Radio Speech Communications

LAJOS HANZO, RAYMOND STEELE, SENIOR MEMBER, IEEE, AND PETER-MARC FORTUNE

Abstract—**A combined subband speech coding (SBC), Bose-Chaudhuri-Hocquenghem (BCH) error-correction coding, and 16-level quadrature amplitude modulation (16-QAM) scheme with switched diversity and speech postenhancement is proposed. The system's performance is dramatically improved by deploying some degree of fade tracking capability over fading channels. Further quality enhancement accrues by using appropriate mapping between the SBC speech codec and the Gray coded QAM words. Various BCH codes are utilized to adequately match the error-correcting power to the perceptual importance of the SBC bits. One of our proposed systems operates at 7 kBd and yields good communications-quality speech for channel signal-to-noise ratios (SNR's) in excess of 20 dB and encounters a maximum overall system delay of 55.125 ms. A more complex arrangement uses second-order switched diversity to reduce both the channel SNR required to around 16 dB and the transmission rate to 5 kBd, when the vehicular speed is 30 mi/h, while the system delay is unchanged at 55.125 ms.**

I. Introduction

ALTHOUGH CURRENT cellular mobile radio systems use analog modulation techniques to transmit speech signals, the next generation systems [1] will use digital modulation in either an FDMA or a narrow-band TDMA format. Because the battery consumption for hand-held portables is severely limited at the present, power amplifiers will operate in class-C, necessitating binary modulation. Looking further into the future, microcellular and macrocellular mobile radio systems will be deployed [2]-[4], as the size of the cells is the most crucial factor in determining spectral efficiency, and hence the number of users that can be accommodated. With the advent of microcells, whose size varies from an office to a 3-km segment of a highway [5], multilevel modulation can be used in conjunction with linear amplifiers.

The transmission of logarithmic PCM via M-level quadrature amplitude modulation (QAM) over Rayleigh fading channels has been studied, both with [6] and without [7] weighting, and with diversity reception. Ideal automatic gain control (AGC) was considered, and no error-correction coding was employed. The results were encouraging and prompted us to examine the specific case of 16-level QAM for subband coded (SBC) speech, with nonideal AGC, and the careful deployment of Bose-Chaudhuri-Hocquenghem (BCH) channel coding as the link between SBC and QAM. We chose 16 kb/s SBC as it is capable of yielding toll quality speech in the presence of a bit-error rate (BER) of 10^{-3} and can be produced on a DSP chip [8]. The choice of 16 levels, i.e., four bits per baud, for the QAM is considered to be realizable and to yield a substantial gain in spectral efficiency over binary modulation. We opt for BCH coding as we know [9], [10] it is a powerful error-correcting code in the mobile channel environment that can correct both random and bursty errors. The major unknown is how to map the SBC data to the QAM modulator via the BCH coder, and the choice of AGC.

We commence our discourse by describing the principles of the 16-level QAM modem in Section II. Its performance is evaluated using both theoretical and experimental techniques via Gaussian and Rayleigh-fading channels. In Section III the performance of various AGC methods is analyzed. Section IV explores the benefits of using 16-QAM constellation distortion, Section V considers the application of diversity techniques, while Section VI is concerned with BCH error correction coding. Finally, in Section VII we propose a number of systems with different attributes.

II. 16-Level QAM

In 16-level QAM the bit stream is suitably assembled into 4-b symbols and each symbol is transmitted by a carrier wave having a unique amplitude and phase. The duration of each symbol determines the bandwidth of the QAM signal. Fig. 1 shows a 16-level constellation where each dot represents the position of the phasor relative to the intersection of the axes marked I (for in phase) and Q (for quadrature). A particular phasor P4 is shown and is seen to be associated with the unique 4-b symbol 0011. If the next input data symbol is 1100, phasor P10 is transmitted, and so on.

The phasors of the 16-level constellation may be decomposed into two independent four-level AM signals that are transmitted on quadrature components of the same carrier. Each AM carrier is transmitted with an amplitude of either $-3d$, $-d$, d or $3d$, where d is the coordinate spacing shown in Fig. 1. The combinations of these quadrature AM carriers form unique points, i.e., phasors, in the QAM constellation. The four-level AM components are binary encoded using two Gray coded bits for each level. Gray codes 01, 00, 10 and 11, are assigned to levels $3d$, d, $-d$ and $-3d$, respectively. Representing the two bits of the

Manuscript received September 12, 1989; revised March 5, 1990.

The authors are with the Department of Electronics and Computer Science, University of Southampton, Southampton 509 5NH U.K.

IEEE Log Number 9038884.

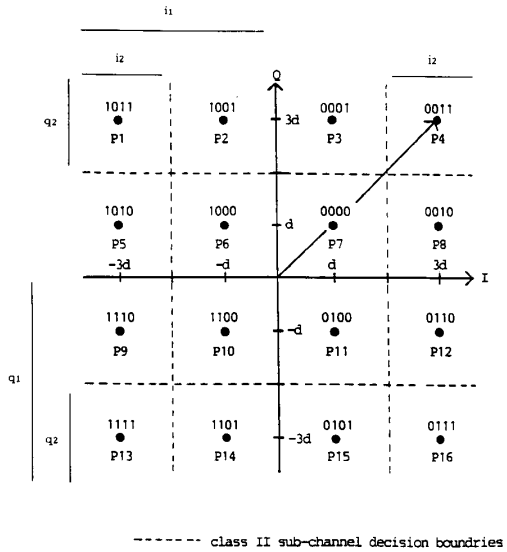

Fig. 1. 16-level QAM constellation.

in-phase code by i_1, i_2 and the quadrature code by q_1, q_2, the 16 QAM phasors are assigned a unique 4-b word by interleaving the most significant and least significant bits of its two component signals forming the word i_1, q_1, i_2, q_2. The Gray code properties ensure that if the receiver erroneously concludes that the transmitted phasor is one of the four neighboring quadrature phasors, the regenerated 4-b symbol has only one of its bits in error.

The demodulation of the received QAM signal is achieved by performing two quadrature AM demodulations. The most significant bit (MSB) of the QAM code word designated by i_1 is regenerated according to

$$\begin{aligned} &\text{if} \quad I \geq 0, \quad \text{then} \quad i_1 = 0 \\ &\text{if} \quad I < 0, \quad \text{then} \quad i_1 = 1 \end{aligned} \tag{1}$$

where I is the received component of the carrier on the in-phase axis. Similarly the second bit q_1 is logically assigned as

$$\begin{aligned} &\text{if} \quad Q \geq 0 \quad \text{then} \quad q_1 = 0 \\ &\text{if} \quad Q < 0 \quad \text{then} \quad q_1 = 1, \end{aligned} \tag{2}$$

where Q is the received component of the carrier on the quadrature-phase axis. The decision boundaries for the third and fourth bits i_2 and q_2, respectively, are shown in Fig. 1. Thus the third bit is regenerated from

$$\begin{aligned} &\text{if} \quad I \geq 2d, \quad \text{then} \quad i_2 = 1 \\ &\text{if} \quad -2d \leq I < 2d, \quad \text{then} \quad i_2 = 0 \\ &\text{if} \quad -2d > I, \quad \text{then} \quad i_2 = 1, \end{aligned} \tag{3}$$

while the fourth bit is formulated by applying

$$\begin{aligned} &\text{if} \quad Q \geq 2d, \quad \text{then} \quad q_2 = 1 \\ &\text{if} \quad -2d \leq Q < 2d, \quad \text{then} \quad q_2 = 0 \\ &\text{if} \quad -2d > Q, \quad \text{then} \quad q_2 = 1. \end{aligned} \tag{4}$$

Once the inequalities (1)–(4) have been evaluated, the bits associated with i_1, i_2, q_1, q_2, are regenerated and the next phasor is processed, and so on. Observe that in the process of demodulation, the positions of the bits in the words associated with each point in the QAM constellation have a profound effect on the probability of them being in error. In the case of the two MSB's the distance from a demodulation decision boundary of each AM component is $3 \cdot d$ for 50% of the time, and d for 50% of the time; assuming that each phasor occurs with equal probability. By contrast, the two least significant bits (LSB) are always at a distance of d from the decision boundary, and consequently the protection distance is decreased by 50% compared to the MSB's. Thus, we may consider our QAM system to have two data subchannels, namely, that associated with the MSB's and that associated with the LSB's. We will refer to the former as a class I (CI) and the latter as a class II (CII) subchannel. Clearly, bits transmitted via the class I subchannel are received with a lower probability of error compared to those bits in the class I subchannel.

A. Performance in the Presence of Gaussian Channel

Consider independent pseudorandom binary sequences (PRB's) to be applied to class I and class II subchannels of the 16-level QAM constellation shown in Fig. 1. The QAM signal is transmitted over an additive white Gaussian noise (AWGN) channel to a receiver that maintains perfect carrier recovery. Demodulation is performed according to (1)–(4). For the least significant bits of the Gray coded QAM words, i.e., those associated with the class II subchannel, a bit error will occur if the noise exceeds d in one direction or $3 \cdot d$ in the opposite direction. Dismissing the latter as insignificant, the probability of a class II bit being in error is

$$P_{\text{IIG}} = Q\left\{\frac{d}{\sqrt{N_0/2}}\right\} = \frac{1}{\sqrt{2\pi}} \int_{d/\sqrt{N_0/2}}^{\infty} \exp\left(-x^2/2\right) dx \tag{5}$$

and N_0 is the one-sided spectral density function of the Gaussian channel noise. As the average symbol energy of the 16-level QAM constellation computed for the phasors $P_1 \cdots P_{16}$ in Fig. 1 is

$$E_0 = 10d^2, \tag{6}$$

we may write

$$P_{\text{IIG}} = Q\left\{\sqrt{\frac{E_0}{5N_0}}\right\}. \tag{7}$$

For class I subchannel data, bits i_1, q_1 are at a protection distance of d from the decision boundaries half the time, and the protection distance is $3 \cdot d$ half the time. Therefore the probability of a bit error is

$$\begin{aligned} P_{\text{IG}} &= \frac{1}{2} Q\left\{\frac{d}{\sqrt{N_0/2}}\right\} + \frac{1}{2} Q\left\{\frac{3d}{\sqrt{N_0/2}}\right\} \\ &= \frac{1}{2}\left[Q\left\{\sqrt{\frac{E_0}{5N_0}}\right\} + Q\left\{3\sqrt{\frac{E_0}{5N_0}}\right\}\right]. \end{aligned} \tag{8}$$

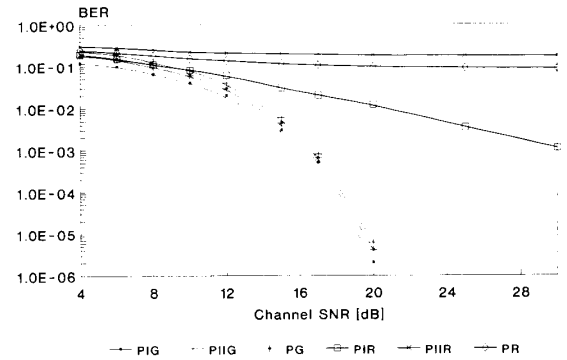

Fig. 2. CI and CII BER variation versus channel SNR.

The probabilities P_{IG} and P_{IIG} as a function of E_0/N_0 are given by (7) and (8) and displayed in Fig. 2. Also shown is the average probability P_G of bit error for the 16-level QAM system as

$$P_G = (P_{IG} + P_{IIG})/2. \tag{9}$$

Simulations where the channel SNR was calculated as the average signal power divided by the average noise power, calculated over the entire simulation period, gave nearly identical curves for P_{IG}, P_{IIG}, and P_G to those computed from (7)–(9). These simulations were done to verify the PRBS and AWGN sources that were required in subsequent simulations. The essential feature of the AWGN performance is that there is only a small advantage in using the class I subchannel over using the class II subchannel.

B. Performance Over a Rayleigh-Fading Channel

Narrow-band mobile radio systems employing conventional size cellular structures are known [11] to have received signal envelopes that have Rayleigh probability density functions (pdf's). In order to be able to transmit SBC speech over these channels we need to know the behavior of class I and II subchannels when pseudorandom binary sequence data are the information source. Accordingly we performed simulations with a Rayleigh fading envelope sampled at 16 k samples/s for a vehicle traveling at 30 mi/h. By up- and down-sampling the Rayleigh-fading envelope we were able to produce a range of envelopes for different vehicle speeds. The propagation frequency was 900 MHz. The other parameters conformed to those in the AWGN experiments.

In contrast to the AWGN channel where there was little difference in BER performance between the two subchannels, the difference became profound when the transmissions were over a Rayleigh-fading channel. The results are presented in Fig. 2. Whereas the BER decreased with increasing channel SNR, reaching 10^{-2} at 20 dB and 10^{-3} at 30 dB, for the class I subchannel; the class II subchannel was virtually independent of channel SNR and above 0.15. Thus the class I subchannel did have an adequate performance for channel SNRs in excess of 20 dB, while the class II subchannel was unusable. When the different BER performances of the subchannels were not exploited, we were faced with a transparent system characterized by the BER curve P_R, which is the average of the class I and class II BERs.

1) Theoretical Analysis of 16-QAM Performance Over Rayleigh-Fading Channels: In this section we investigate the system performance over a nonfrequency-selective fading channel, where the signal bandwidth is much lower than the coherence bandwidth of the channel. Therefore, all frequency components of the transmitted signal undergo the same attenuation and phase shift. The multipath components in the received signal are not resolvable and the channel transfer function is given by

$$c(t) = \alpha(t) \cdot e^{-j\Phi(t)}, \tag{10}$$

where $\alpha(t)$ represents the Rayleigh-fading envelope and $\Phi(t)$ the phase of the channel, which is uniformly distributed over $[-\Pi, \Pi]$. If additionally the fading is slow, so that $\alpha(t) = \alpha$ and $\Phi(t) = \Phi$ for the duration of one signaling interval, the received signal $r(t)$ at the channel's output is

$$r(t) = \alpha \cdot e^{-j\cdot\Phi} \cdot m(t) + n(t), \tag{11}$$

where $m(t)$ is the transmitted modulated signal and $n(t)$ is an AWGN process. On rewriting (7) and (8) derived for class I and class II subchannels as a function of E_0/N_0 for AWGN channels in terms of the instantaneous SNR γ via Rayleigh-fading channels, we get:

$$P_{IR}(\gamma) = \frac{1}{2}\left[Q\left\{\sqrt{\frac{\gamma}{5}}\right\} + Q\left\{3\sqrt{\frac{\gamma}{5}}\right\}\right], \tag{12}$$

and

$$P_{IIR}(\gamma) = Q\left\{\sqrt{\frac{\gamma}{5}}\right\}. \tag{13}$$

As the fading envelope is changing from one signaling interval to another, the instantaneous SNR γ is also changing, as the noise power N_0 is fairly constant but the received signal energy E_0 is fading. The average BER is found by calculating the bit-error probability at a given instantaneous SNR γ and averaging it over all possible SNR's. This is carried out by multiplying the bit-error probability $P(\gamma)$ at the instantaneous SNR γ with the occurrence probability of the specific SNR γ expressed in terms of its probability density function $C(\gamma)$ and then averaging, i.e., integrating this product over all possible values of γ:

$$P_{be} = \int_0^\infty P(\gamma) \cdot C(\gamma)\, d\gamma. \tag{14}$$

The computation of P_{IR} and P_{IIR} is somewhat lengthy, so the interested reader is referred to the Appendix for the derivation of the CI and CII BER formulas given as follows:

$$P_{IR}(\Gamma) = \frac{1}{2\Gamma}\int_0^\infty \left[Q\left\{\sqrt{\frac{\gamma}{5}}\right\} + Q\left\{3\sqrt{\frac{\gamma}{5}}\right\}\right] \cdot e^{-\gamma/\Gamma}\, d\gamma. \tag{15}$$

$$P_{II,R}(\Gamma) = \frac{1}{2\Gamma}\int_0^\infty Q\left\{\left(\frac{2\bar{\alpha}}{\alpha} - 1\right)\sqrt{\frac{\gamma}{5}}\right\} e^{-\gamma/\Gamma}\, d\gamma + \frac{1}{2\Gamma}\int_0^\infty Q\left\{\left(\frac{3\bar{\alpha}}{\alpha} - 2\right)\sqrt{\frac{\gamma}{5}}\right\} e^{-\gamma/\Gamma}\, d\gamma. \tag{16}$$

Here the average SNR Γ is defined as the expectation of the instantaneous SNR γ, i.e., $\Gamma = \bar{\gamma}$ and $\bar{\alpha}$ is the expectation of the Rayleigh-fading envelope α defined in the context of (11).

When we evaluated the CI and CII bit-error probabilities from (15) and (16), respectively, we received nearly identical curves to those depicted in Fig. 2 from our simulations.

III. AGC Methods for QAM

Our approach to enhancing the BER performances of the CI and CII subchannels is to implement some degree of channel equalization in the form of an automatic gain control. By decreasing the BER to an acceptable level, practical error-coding techniques can be successfully deployed. Our AGC arrangements use either forced updating, or a method based on the continuous time averaging of the received QAM phasors.

A. Forced Updating AGC

This technique is essentially channel sounding. Every k symbol of the transmitted data is followed by a sounding symbol selected to yield a QAM phasor of maximum amplitude, e.g., either phasor P1, P4, P13 or P16 in Fig. 1. At the receiver the received sounding symbols are separated from the data and fed to an AGC system which calculates the amplification or attenuation

$$G = R/3\sqrt{2}\,d$$

necessary to modify the received phasor R to the expected signal level, say $R1$. This value of G is then applied to the incoming k QAM phasors enabling QAM demodulation to ensue against a constellation whose dimensions are the same as those used in the QAM modulator.

The smaller the value of k, the lower the probability of symbol error, but the transmission overhead is increased. Too low a value of k seriously decreases the gain in spectral efficiency conferred by the multilevel modulation process. The penalty inflicted by the introduction of the sounding symbols could be mitigated by using two bits of the sounding symbols for data transmissions and exploiting the fact that the phasors P_1, P_4, P_{13}, and P_{16} having maximum amplitudes differ only in their two MSB's, hence one would lose only the two LSB's.[1]

B. Average Locking

An alternative technique that avoids the insertion of extra symbols into the data stream was sought. The method adopted, called average locking, computes the arithmetic mean square value R of the previous k phasors and compares this average with the expected mean square value E_0 of the 16-level QAM signal. As all symbols are transmitted with equal probability, $E_0 = 10d^2$. The phasor R to be demodulated is scaled by the ratio of these values, namely,

$$G = \sqrt{E/\hat{R}}$$

and demodulation follows.

[1] Comment of the reviewer.

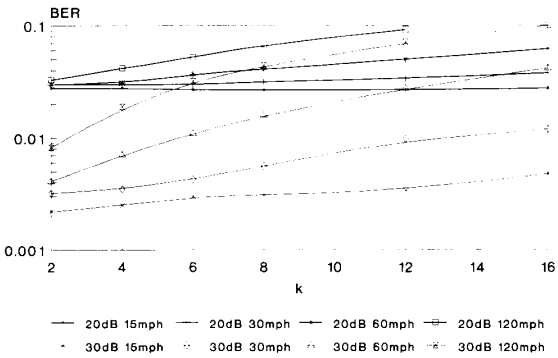

Fig. 3. CII BER versus k with forced updating AGC.

C. BER Performance of the CII Subchannel Using AGC

The performance of forced up-dating and average locking was investigated using simulations for various channel SNRs over a range of k values. Neither AGC method significantly altered the BER or the class I subchannel.

Our attention was therefore focused on the class II subchannel performance. Fig. 3 shows the variation of the class II BER as a function of k when forced updating was used, the channel SNR was either 20 or 30 dB and the vehicular speeds ranged from 15–120 mi/h. These class II subchannel simulations were performed so that for each sample of the 30 mi/h Rayleigh fading envelope one QAM sample was transmitted. The transmission rate was therefore 16 kBd. Thus a curve in the figure corresponding to 120 mi/h was equivalent to one at 60 mi/h when the transmission rate was 8 kBd. As expected, the BER became progressively smaller as k decreased, but the transmission overhead to convey k to the receiver became prohibitively large. As the vehicular speed increased, the ability of the AGC to track the fade decreased. For low values of k a 10 dB improvement in channel SNR resulted in the BER being reduced by up to an order of magnitude.

The corresponding curves for the average locking AGC are displayed in Fig. 4. We observed that for both channel SNR's investigated, namely for 20 and 30 dB, there was an optimum value of k for each speed. For the lower SNR of 20 dB the optimum k varied over a wide range with speed, but the corresponding variation of BER was relatively small. At the higher SNR of 30 dB the variations of the BER with the optimum k were much larger, but the range of k was smaller. In subsequent sections we employ the average locking AGC system as its performance matches that of the forced update AGC, without the necessity of transmitted side information. Operating with channel SNR's in excess of 22 dB, we decided to use a fixed k of four because when the SBC (discussed in Section VII-A) in conjunction with QAM operates at 6.7 kBd with vehicular speeds of 30 and 50 mi/h, the equivalent curves in Fig. 4 would be curves at $60 \times 8/6.7 = 72$ and $120 \times 8/6.7 = 144$ mi/h.

IV. 16-QAM Constellation Distortion

As seen in Section III, the AGC methods significantly lower the BER of the CII subchannel, but do not affect that of

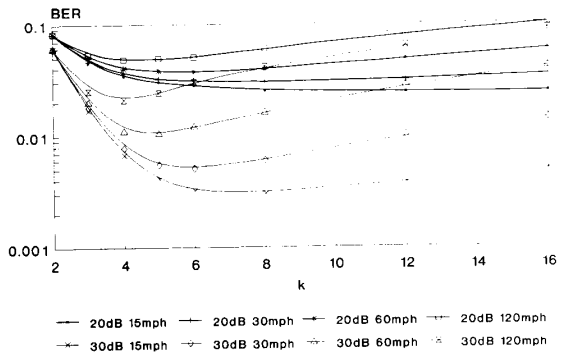

Fig. 4. CII BER versus k with average locking AGC.

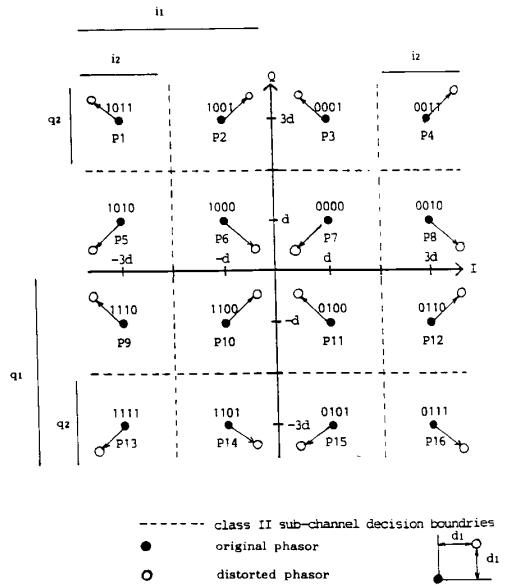

Fig. 5. 16-QAM signal constellation distortion scheme.

the CI subchannel. However, as the BER of the CI subchannel is still lower than that of the CII subchannel, we first explore the possibilities of equilizing them. This renders both subchannels equivalent and results in a transparent system.

A plausible way of equalizing the BER performances of the CI and CII subchannels is to distort the original signal constellation. This is carried out by moving the constellation phasors symmetrically nearer to their respective CI decision boundaries and ensuring higher protection distance for the bits of the CII subchannels, as shown in Fig. 5. We define the constellation distortion factor CD as

$$\mathrm{CD} = 20 \lg \frac{d}{d - d_1} \quad [\mathrm{dB}],$$

where d_1 represents the protection distance reduction, caused by shifting the constellation points symmetrically toward both of their CI decision boundaries. The CI and CII subchannel BER's at SNR = 20 dB are depicted in Fig. 6 as a function of CD, where we observe that around CD = 3.5 dB the two subchannels have identical BER's, but their average is also

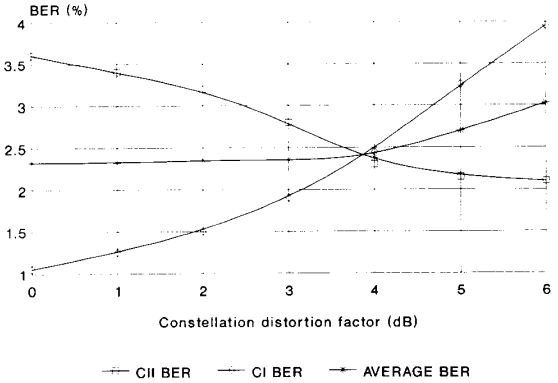

Fig. 6. BER of CI and CII subchannels versus constellation distortion factor (dB).

slightly increased to 2.5%. In this way we arrive at a system with two identical subchannels, which nevertheless is still unsuited for the transmission of SBC speech. However, the resulting BER = 2.5% is now sufficiently low to be decreased still further by BCH coding.

In summary, using constellation distortion with a distortion factor of CD = 3.5 dB we arrive at a transparent system with equivalent CI and CII subchannels, which does not require any special mapping strategy for the protection of particularly important speech information bits. Consequently, it is sufficient to use only one BCH codec to remove the channel errors, yielding a simple system. However, a system exploiting the BER differences of the CI and CII subchannels, rather than equalizing them, can provide a better overall performance at the price of slightly increased complexity.

V. Diversity Techniques

To enhance the CI and CII subchannel's BER performance we deployed switched diversity. Our simulation results with dth order diversity confirmed the effectiveness of the action for combating channel fading. Each of the d received signals was generated by modifying the transmitted phasor by the Rayleigh-fading envelope, using a different, random starting point. Also a separate AWGN source was used for each incoming signal. Each of the d received signals was assigned a separate average locking AGC sytem, and at each sampling instant the channel exhibiting the highest average signal level over the interval $k = 4$ was selected for 16-QAM demodulation.

The 16-QAM CI and CII subchannel's logarithmic BER is displayed in Fig. 7 for the SNR values of 20, 22, and 25 dB, respectively, as a function of the diversity order d. While the CII subchannel's BER performance was hardly effected by deploying diversity, the CI subchannel performance was decreased by two orders of magnitudes, when the diversity order was $d = 4$. Even for the more practical second-order diversity the CI subchannel BER was decreased below 0.1% for an SNR = 20 dB. Hence, the CI subchannel was well suited for SBC speech transmission, while the BER = 2% of the CII subchannel can be tackled by BCH coding to allow for good quality speech communication.

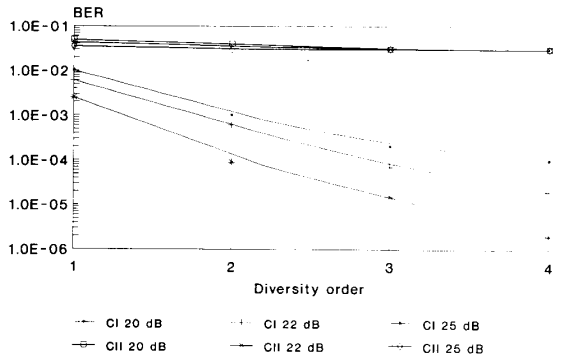

Fig. 7. CI and CII BER versus diversity order via Rayleigh channel.

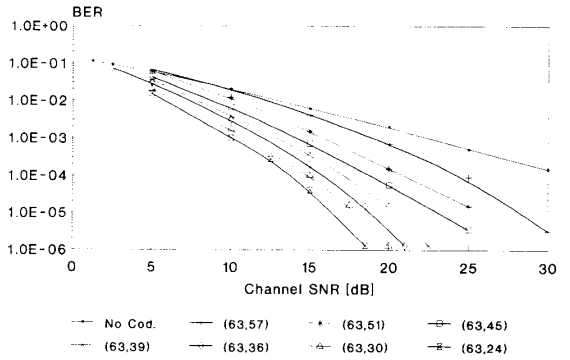

Fig. 8. Decoded BER of BCH codes versus channel SNR with BPSK modulation.

VI. Selection of Error Correction Codes

With the incentive of finding the best error-protection schemes for mobile speech communications we have carried out investigations [9], [10] using a variety of forward error-correction codes and interleavers. BCH and Reed–Solomon (RS) block codes combined with interleavers are powerful in combating bursty errors, particularly if the demodulator cannot supply channel measurement information. Long Reed–Solomon codes are convenient because of their capability of "overbridging" long channel fades, and hence they do not require interleavers to disperse bursty errors. However, their complexity grows proportional to $6t^2$, where t is the number of nonbinary symbols correctable by an RS(n, k, t) code, assuming a Berlekamp–Massey decoder is used. Furthermore, the long codes incur long system delays. Therefore, shorter codes combined with interleavers result in reduced complexity, while maintaining nearly identical error-correcting power.

Due to their maximum minimum distance property RS codes possess a very high maximum error correcting capability. Specifically, a t symbol correcting RS code can theoretically correct up to $t.m$ number of bit errors, where m is the number of bits in an RS coded symbol. In practice, however, the average number of bit errors in a symbol depends on the symbol size, but it is seldom more than 1.5–2 b/symbol. Therefore, binary BCH codes often outperform RS codes. A further advantage of the BCH codes is that due to their binary natures computing the positions of the errors in a codeword concludes the error correction, as the appropriate bit simply has to be inverted. In the nonbinary RS codes a further step is required to compute the magnitude of the errors, for example, by using Forney's algorithm.

In summary, in this application we opt for BCH codes of a moderate wordlength of 63. The error correcting power of a set of BCH codes is represented by Fig. 8, where the effective decoded BER is depicted as a function of channel SNR when BPSK modulation transmissions occur over Rayleigh-fading channels. In this figure we use channel SNR for comparison, rather than E_b/N_0, where E_b represents the bit energy and N_0 the noise spectral density. This is because we are concerned with decoded BER for a given channel condition, rather than with coding gain. We have chosen BPSK modulation in this experiment for the assessment of BCH code performances to limit the variety of scenarios, since over 16-QAM the decoded BER depends also on the subchannel investigated.

The codes preselected for investigation are:

BCH(63,57,1)
BCH(63,48,2)
BCH(63,45,3)
BCH(63,39,4)
BCH(63,36,5)
BCH(63,30,6)
BCH(63,24,7).

Their coding rates range from $R = 0.4$ to $R = 0.9$ providing a wide variety for deployment in the CI and CII 16-QAM subchannels.

VII. Proposed SBC/BCH/16-QAM Systems

The system's block diagram is depicted in Fig. 9. The subband coded speech is mapped in the block "SBC MAP" into groups CI and CII. The bit streams in both classes are then appropriately BCH encoded and interleaved in the blocks "BCHE" and "INT," respectively. The dashed lines in the upper branches of both encoder and decoder together with the "diversity" block indicate that these system elements are optional. Namely, in one of our proposed systems second-order switched diversity is utilized to reduce the BER of the class I subchannel to a value where no error-correction coding is required by the SBC, as suggested by Fig. 7. The BCH encoded and interleaved subchannels are then assembled by the block "ASM QAM" for modulation in the appropriate CI or CII subchannel. After "QAM" modulation, transmission via the fading channel "Chan" and QAM demodulation "QAMD," the subchannels are disassembled in the block "DASM QAM." Then the subchannels are deinterleaved in "DEINT" and decoded by "BCHD," before demapping is carried out in "SBC DEMAP" to reinstall the SBC bits in their original positions. The error-detecting capability of the BCH decoder used to protect the most significant SBC bits is exploited to invoke a speech postprocessing algorithm, if the received speech information is deemed to be seriously corrupted.

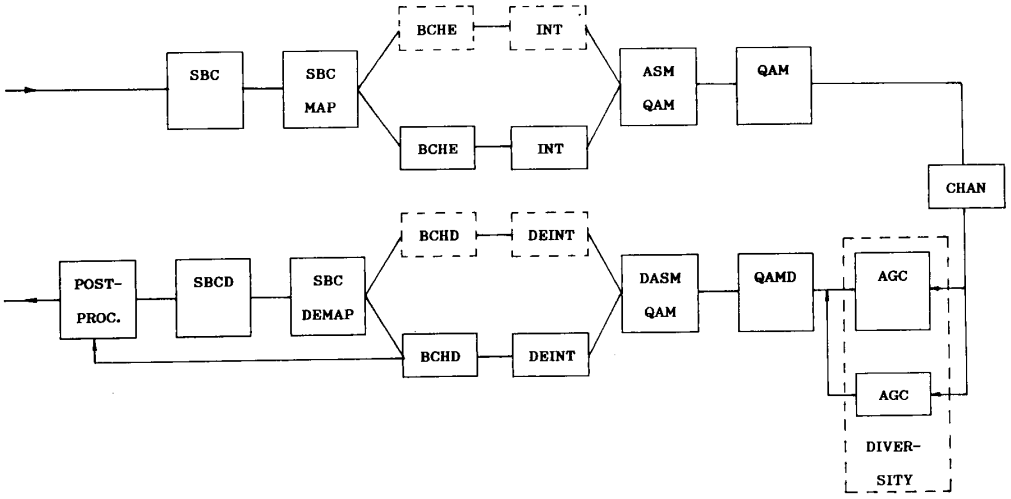

Fig. 9. System's block diagram.

TABLE I
SEMI-ADAPTIVE SBC BIT ALLOCATION

SUB-BAND KHz	0.0 - 0.5	0.5 - 1.0	1.0 - 1.5	1.5 - 2.0	2.0 - 2.5	2.5 - 3.0	3.0 - 3.5	3.5 - 4.0
CLASSIFICATION	BIT ALLOCATION							
VOICED	4	4	3	2	2	0	0	0
INTERMEDIATE	4	3	2	2	2	2	0	0
UNVOICED	2	3	3	3	2	2	H	0
VOICE BAND DATA	0	0	4	4	4	3	0	0

H means high frequency band regeneration

Based on our previous studies [8], [17] and present deductions, a number of combined SBC/BCH/16-QAM systems with various speech qualities and transmission rates can now be contrived. As an objective quality measure for system comparison the SBC segmental SNR (SEGSNR) is used, and in error-free conditions the SBC has a SEGSNR of 14 dB. When the speech is corrupted by channel impairments, in our SBC implementation a SEGSNR = 10 dB or better is associated with good communications quality subjective assessment [8].

As the SBC codec has a transmission rate of 16 kb/s, then if no BCH coding is deployed, the resultant transmission speed via 16-QAM is 16 kb/s/4 = 4 kBd. However, this system is not capable of delivering good communications quality speech, as is evident by the SEGSNR curve in Fig. 11. This system is merely used as a benchmark for our candidate schemes.

Another system can be devised by equalizing the BER's of both subchannels by the help of constellation distortion with CD = 3.5 dB, but because of the 2.5% BER at SNR = 20 dB, at least a half-rate BCH code has to be utilized. This results into an 8 kBd system having relatively low complexity with no mapper and only one BCH codec.

To exploit the BER difference between the subchannels, we deploy BCH coding with different coding rates for the two subchannels to equalize the BER differences after BCH decoding. Alternatively, we use the subchannels as two independent systems, and arrange for the perceptually and objectively important SBC speech bits to be transmitted over the better subchannel.

A. The Subband Codec

The subband codec [8] produces eight subbands each of 500 Hz bandwidth by means of a quadrature mirror filter (QMF) bank. Each subband signal is encoded using Jayant's one-word memory quantiser whose number of bits is either 0, 2, 3 or 4, depending on which signal classification is used. The classification, given in the first column in Table I, is determined by the distribution of spectral energy in the speech signal, measured in terms of the signal power ratios at various QMF output stages. If, for example, voiced speech is deemed to be present, the QMF output signals beyond 2.5 kHz are always assigned zero bit. Should, however, an unvoiced classifier be received by the decoder, it automatically assumes that two bits have been deployed to encode the subband 2.5–3 kHz, etc. The orders of the FIR QMF stages

are 32, 16, and 12 in the first, second, and third bandsplitting operation, respectively, whence the delay introduced in the filters is computed to be 13.125 ms.

Eight input speech samples with a sampling frequency of 8 kHz are received in 1 ms and produce one sample at each QMF output. This results in 15 b being produced from the subband quantizers according to Table I and yields a rate of 15 kb/s as each subband is sampled at 1 kHz. The bit allocation is reviewed every 6 ms, and the classification adopted is represented by a 2-b word that is repeated twice more for channel protection. Thus a SBC frame consists of $(6 \times 15) + 6 = 96$ bits with a duration of 6 ms.

In this particular SBC implementation the semi-adaptive bit allocation scheme of Table I was used, and for a particular classifier it was relatively straightforward to find the most important SBC bits. Because it is a huge task to perceptually investigate the sensitivities of all SBC bits, common practice is to use the SEGSNR and the cepstral distance objective measures to assess bit sensitivities [14], [15]. Although the cepstral distance is considered to have the highest correlations with subjective speech quality measures [16], in harmony with [15], we have found it meaningful only when assessing the sensitivities of linear predictive spectral parameters. Therefore we rely in our experiments entirely on the SEGSNR degradations caused by the individual SBC bits.

The SBC bit-error sensitivity measurements have been carried out by systematically corrupting one of the 15 bits to evaluate the SEGSNR degradation caused. The results are depicted in Fig. 10 for the case of a "voiced" classifier. The error-free SEGSNR = 14 dB, as mentioned earlier. The most sensitive bit was the fourth one in the 15-b block, representing the second subband MSB (see Table I), which, when corrupted, resulted in an SEGSNR of −5.6 dB. The least important SBC bit was bit five, which reduced the SEGSNR to only 10.8 dB, when systematically corrupted. In this fashion all the SBC bits were ordered according to their objective importance for each SBC classifier, as summarized in Table II. Clearly, the most sensitive bits had to be transmitted via the better subchannel in our system. Therefore the SBC mapper in Fig. 9 always mapped them according to this criterion.

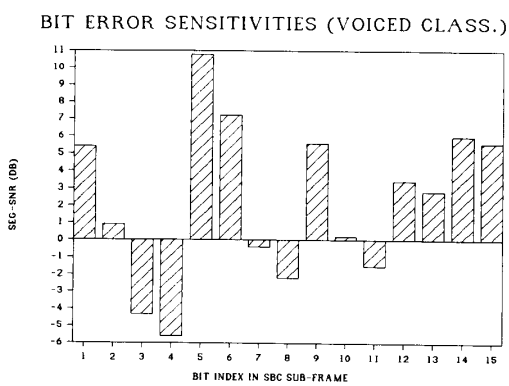

Fig. 10. Bit-error sensitivity versus bit index for voiced SBC classifier.

B. The 7-kBd System

The philosophy behind this system is to add channel coding to both subchannels in such a way that the BER of each is not only low enough to carry toll-quality SBC speech, but also nearly matched. As a consequence no special mapping strategies are required. In the absence of BCH coding, but in the presence of average locking AGC, the BER for the CII subchannel is approximately three times that encountered in the CI subchannel. Therefore, we select the BCH code for the CII subchannel to have approximately three times the error correcting capability of the BCH code used for the CI subchannel. Because the total protected data rate passing via each of the subchannels must be equal, the redundancy of the code used with the CI subchannel must be matched to that used in the CII subchannel.

Conveniently, the BCH(63,48,2) code and the BCH(63,24,7) code constitute an appropriate choice both in terms of their redundancy rates and error correcting powers (see Fig. 8). A block of six 6-ms long SBC frames is buffered to give 576 bits to be encoded. Then the SBC mapper (see Fig. 9) splits this block into two contiguous frames of $6 \times 64 = 384$ CI bits and $6 \times 32 = 192$ CII bits. In other words, every third bit is placed into the CII stream and the other two are sent into the CI stream. The BCH(63,48,2) CI encoder generates out of $8 \times 48 = 384$ bits $8 \times 63 = 504$ encoded bits. Similarly, the BCH(63,24,7) CII encoder produces out of $8 \times 24 = 192$ bits $8 \times 63 = 504$ bits. In other words, in both subchannels 504 bits, consisting of eight BCH encoded frames are transmitted. As six SBC frames are processed at a time, the total system delay is constituted by the $6 \times 6 = 36$ ms interleaving delay, plus the 13.125 ms algorithmic QMF delay as well as a 6 ms real-time processing delay. The total transmission rate is 1008 b/36 ms = 28 kb/s = 7 kBd, since during six SBC frames, i.e., 36 ms, eight BCH frames are assembled. Interleaving is carried out over eight BCH encoded frames using a block diagonal interleaver [9]. The system's performance over Rayleigh-fading channels is depicted in Fig. 11 for final system comparison.

In summary, using the 7-kBd system good communications quality speech is obtained for channel SNR's in excess of 20 dB for a vehicular speed of 30 mi/h. Due to appropriate BCH coding and interleaving similar performance is achieved at half and double vehicular speeds, i.e., at 15 and 60 mi/h.

C. The 5-kBd System

The philosophy behind this system is that rather than trying to equalize the BER performances of the CI and CII subchannels, we exploit their different integrities. Namely, a more bandwidth efficient system can be designed if we arrange for the more important SBC bits to be transmitted via the better subchannel and for the less important ones to travel via the worse subchannel. The CI subchannel having a higher BER performance than CII can be used to transmit the group of more important SBC bits even for channel SNR's in excess of 20 dB without FEC coding. In the same channel SNR region the CII subchannel can be rendered suitable for the transmission of the less significant SBC bits. Namely, most of the

TABLE II
SBC BIT-ERROR SENSITIVITIES (INDEX 1 REPRESENTS THE HIGHEST SENSITIVITY)

Sensitivity / Classifier	1	2	3	4	5	6	7	8	9	10	11	12	13	14	15
Voiced	4	3	8	11	7	10	2	13	12	1	15	9	14	6	5
Unvoiced	1	2	8	5	7	11	6	13	12	4	10	15	14	9	3
Intermediate	4	3	9	8	7	11	6	10	13	12	5	2	15	14	1

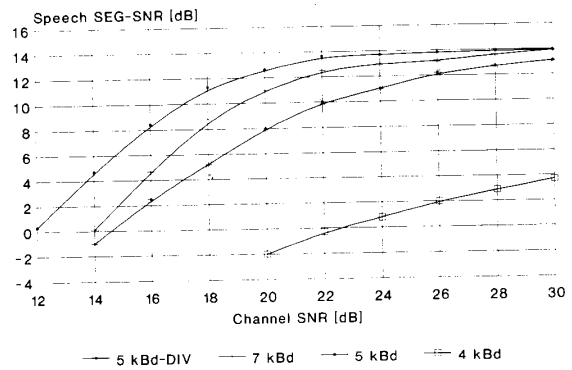

Fig. 11. SEG-SNR of various SBC/BCH/QAM systems versus channel SNR.

channel errors can be corrected by using a powerful, appropriately shortened BCH(60,36,4) code combined with an interleaver. This code has been selected to provide approximately 95% error correction probability and to match our special bit-packing requirements. This means that for 95% of the time all the CII bits are corrected in the BCH coded frames, and for 5% of the time the code's error correcting capability is overloaded. In these situations the code's error detecting capability is exploited to invoke an analog speech postenhancement technique described later in this section.

Let us first embark on the derivation of the appropriate SBC bit mapping scheme. It is quite crucial that the subband signal's MSB's not be corrupted, and we have seen in Table II that in some subbands the second MSB's are more important than the MSB's of others. As the CII subchannel is now BCH coded, its real throughput is reduced by the amount of redundancy used, but the channel capacity of the CI subchannel is fully exploited. When using the binary BCH(60,36,4) code, 36 least significant SBC bits are encoded into 60 bits and the remaining 60 most important SBC bits of a 96-b SBC frame are sent unprotected via the high integrity CI subchannel. Therefore the SBC mapper has to segregate 60 SBC MSB's by using the bit sensitivity table (Table II). Firstly, the six classifier bits are sent to the group of MSB's. Then the nine most sensitive SBC bits of a 15-b subframe generated each ms are selected in six consecutive such subframes, giving a further 54 MSB's to be transmitted via the CI subchannel. With the proviso that the first six bits of a 96-b SBC frame are always MSB's, the group of the other 54 MSB's are encircled in Table III in case of the "voiced" speech classification. For the "intermediate," "unvoiced" and "voice band data" classification only the MSB's are listed in subtables b, c, and d, respectively. Observe that in harmony with our expectations usually the subband MSB's and second MSB's have to be transmitted via the CI subchannel.

The baud-rate is computed as follows: the original 16 kb/s stream is split into two separate sequences with transmission rates of $16 \times 60/96 = 10$ kb/s and $16 \times 36/96 = 6$ kb/s, respectively. The 6 kb/s rate stream is encoded using the BCH(60,36,4) code into another 10 kb/s sequence resulting in an overall transmission rate of 20 kb/s, or 5 kBd.

This system does not encounter any additional delay introduced by the mapping and BCH coding. It is known, however, that the FEC performance is drastically improved when utilizing interleaving over the interval of the maximum acceptable speech delay. An interleaving depth of eight constitutes the best compromise between BER performance, i.e., speech robustness and system delay. This interleaving period is long enough to "overbridge" most of the fades of a mobile channel in the 900 MHz band, when traveling at vehicular speeds in excess of 15 mi/h. The resultant overall system delay is given by the sum of the $6 \times 6 = 36$ ms interleaving delay, 13.125 ms algorithmic QMF delay as well as 6 ms real-time processing delay, as explained for the 7 kBd system. This 55.125 ms delay can be shortened to 37.125 ms using an interleaving depth of four at the price of slightly reduced robustness.

The overall system's performance is characterized again in terms of speech segmental SNR in Fig. 11 for a vehicle traveling at 30 mi/h. Notice that at the price of approximately 2 dB higher channel SNR requirement a dramatically increased bandwidth efficiency is achieved, when compared with the 7 kBd system. The 5 kBd system guarantees good communications quality speech for channel SNR's in excess of 20–22 dB.

A further drastic system improvement can be achieved if we bear in mind the remarkable CI BER reduction achieved by deploying second-order diversity, as seen in Fig. 7. This approach is particularly advantageous, as the SBC MSB's are carried via the CI subchannel and the majority of the SBC bits (62.5%) are carried over this high integrity route. The SEGSNR performance when using second-order diversity is also depicted in Fig. 11. Observe that in this way the 5 kBd

TABLE III
SBC MAPPING SCHEME FOR EMBEDDED BCH CODING

CLASSIFICATION	SUB-BANDS IN kHz				
	0.0 - 0.5	0.5 - 1.0	1.0 - 1.5	1.5 - 2.0	2.0 - 2.5
VOICED (a)	7 (8) (9) (10)	11 12 (13) (14)	15 (16) (17)	(18) (19)	20 21
	22 (23) (24) (25)	26 27 (28) (29)	30 (31) (32)	(33) (34)	35 36
	37 (38) (39) (40)	41 42 (43) (44)	45 (46) (47)	(48) (49)	50 51
	52 (53) (54) (55)	56 57 (58) (59)	60 (61) (62)	(63) (64)	65 66
	67 (68) (69) (70)	71 72 (73) (74)	75 (76) (77)	(78) (79)	80 81
	82 (83) (84) (85)	86 87 (88) (89)	90 (91) (92)	(93) (94)	95 96
	ONLY CIRCLED NUMBERS LISTED IN SUB-TABLES (b) - (d)				
INTERMEDIATE (b)	9 10 12 13 14 15 16 17 19 24 25 27 28 29 30 31 32 34 39 40 42 43 44 45 46 47 49 54 55 57 58 59 60 61 62 64 69 70 72 73 74 75 76 77 79 84 85 87 88 89 90 91 92 94				
UNVOICED (c)	7 8 11 12 13 14 16 17 19 22 23 26 27 28 29 31 32 34 37 38 41 42 43 44 46 47 49 52 53 56 57 58 59 61 62 64 67 68 71 72 73 74 76 77 79 82 83 86 87 88 89 91 92 94				
VOICE BAND DATA (d)	8 9 10 12 13 14 17 18 21 23 24 25 27 28 29 32 33 36 38 39 40 42 43 44 47 48 51 53 54 55 57 58 59 62 63 66 68 69 70 72 73 74 77 78 81 83 84 85 87 88 89 92 93 96				

system outperforms the 7 kBd scheme and provides good communications quality speech for channel SNR's in excess of 18 dB.

A salient feature of the 5 kBd systems proposed is that the group of SBC MSB's is always mapped onto the CI 16-QAM subchannel. Apart from the perceptual benefits gained, this has a further crucial aspect. Namely, the operation of the average locking AGC is based on the fact that random information with statistically sound average energy is received. Should this not be the case, the AGC does not achieve the predicted performance. When SBC speech is the input data, the MSB's are not perfectly uncorrelated. In other words, the SBC code has redundancy, inherent in the speech, as opposed to some of the more efficient lower bitrate codecs. Therefore if the MSB's are transmitted via the CII subchannel, the average locking AGC performs less favourably than with random signals. This results into a CII BER performance that cannot be controlled efficiently using the same BCH(60,36,4) code. A more powerful code is needed, which reduces the bandwidth efficiency.

It is worth mentioning that we have contrived a very similar 5 kBd system using a Reed-Solomon code over Galois field (GF) 256. The code selected is the RS(60,36,14) code, which can correct 14 errors by encoding 36 eight bits symbols into 60 symbols. In terms of bits, it encodes 288 bits into 480 bits, and therefore eight 96-b SBC frames have to be encoded simultaneously to provide sufficient information (8 $\times$ 36 = 288 bits) for a single codeword. This scheme has the same delay (48 ms) as our BCH coded system with an interleaving depth eight, without necessitating interleaving. Furthermore, it provides slightly more flexibility in the error distribution before code-overloading occurs. According to our simulations the decoded BER performance of the RS(60,36,14) code is slightly inferior to that of the interleaved BCH(60,35,4) code. Therefore the speech SEGSNR is slightly lower than that of the BCH coded system, although the decoding complexity of the RS(60, 36, 14) code is considerably higher. This is due, in the case of the nonbinary RS code, that after computing the error positions in the codewords by the Berlekamp-Massey algorithm the nonbinary error magnitudes have to be determined by using the Forney algorithm [18]. When using binary BCH codes this second step is not required. In addition, shorter codes correcting a lower number of errors generally require a lower number of computations.

D. Speech Postenhancement

In speech communications it is wasteful to deploy FEC codecs designed for worst-case BER conditions, because for most of the time their error correcting power is not required. Digital speech signals, depending on the type of the codec used, can usually tolerate moderate bit-error rates.

Now BCH and RS codes are known to have reliable error detection capabilities [10], particularly if the code in question has powerful error correcting capability. Both the BCH(63,24,7) and BCH(60,36,4) codes used in the CII subchannels in our experiments can detect overloading of the error correcting power with a confidence level in excess of 99%. They can, therefore, be used to reliably detect error bursts in conditions where the received speech waveform is so badly impaired that the postenhancement algorithm should be invoked. We used postenhancement whenever three consecutive SBC frames are erroneously recovered due to BCH decoding failures.

Our speech postprocessing arrangement can be conveniently explained with reference to Fig. 12. An 18-ms section of the decoded SBC speech is shown missing in Fig. 12(a) due to the BCH decoder flagging three consecutive code overloads. We replace this missing speech using the approach of Goodman *et al.* [19] for packet switched speech. Specifi-

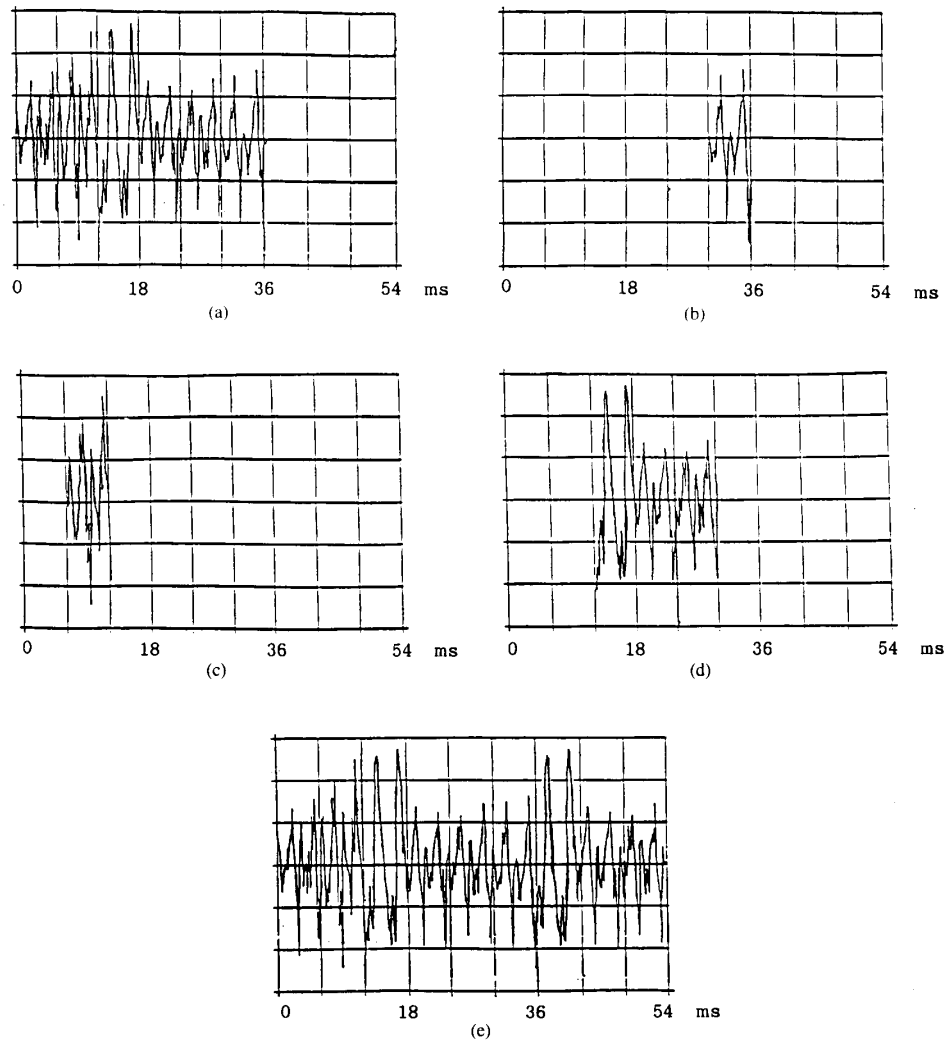

Fig. 12. Speech postenhancement using waveform substitution technique. (a) Delete corrupted speech segment. (b) Identify preceding template. (c) Find the template's match. (d) Select the sequency following the match. (e) Substitute replica.

cally, the speech of 6-ms duration equal to one SBC block immediately preceding the missing frame is used as a template (see Fig. 12(b)) and slid back in time along the search window comprising the previously recovered 36-ms long speech segment. The cross correlation between the template (6 ms) and the momentarily "covered" speech in the search window (36 ms) is computed, and the particular part of the speech in the window associated with the highest cross correlation is noted (see Fig. 12(c)). The rejected frame of speech is now replaced by the 18-ms segment, commencing with the block identified in the correlation search process. Figs. 12(c), 12(d), and 12(e) show the position of the template to give the maximum cross correlation, the frame of speech to be substituted, and the recovered speech after substitution, respectively.

A refinement is to smooth the substituted frame in the recovered speech signal at its edges by employing a raised cosine weighting function. The merging interval includes eight samples of the substituted speech and eight of the error-free speech at each of the two frame boundaries.

VIII. Conclusion

The transmission of 16 kb/s SBC speech via 16-level QAM has been investigated. With the aid of an average locking AGC system and a mapper employing BCH coding, with an option to use second-order diversity, we are able to provide good communications-quality speech at transmission rates of 7 and 5 kBd. The maximum overall system delay for both systems is 55.125 ms. Using half the interleaving period the maximum overall system delay can be reduced to 37.125 ms at the expense of slightly reduced robustness. The channel SNR needs to exceed 18–20 dB, a number easily realizable in the microcellular structures to be used in the next generation of digital mobile radio systems.

APPENDIX

COMPUTATION OF P_{IR} AND P_{IIR} GIVEN IN (15) AND (16)

To determine the average BER's P_{IR} and P_{IIR} over a Rayleigh-fading channel we have to substitute the error probability $P(\gamma)$ for a given instantaneous SNR γ and the PDF $C(\gamma)$ into (14). The instantaneous SNR γ is given in terms of the envelope fading α and E_0/N_0 as follows:

$$\gamma = \alpha^2 \frac{E_0}{N_0}. \tag{17}$$

Since the distribution $C(\alpha)$ of α is known to be Rayleigh, the distribution $C(\gamma)$ of the transformed variable γ is computed by the following theorem [12].

Theorem: Let α be a continuous random variable with the PDF $C(\alpha)$, and let $\gamma = \alpha^2 E_0/N_0$ be a transformation of α. To determine the PDF of γ, $C(\gamma)$ we solve the equation $\gamma = \alpha^2 E_0/N_0$ for α in terms of γ. If α_1 and α_2 are all the real solutions, then:

$$C(\gamma) = C(\alpha_1) \cdot \left| \frac{d\alpha_1}{d\gamma} \right| + C(\alpha_2) \cdot \left| \frac{d\alpha_2}{d\gamma} \right|. \tag{18}$$

The Rayleigh distributed PDF of α is given by

$$C(\alpha) = \left(\frac{\alpha}{\alpha_0^2} \right) e^{-\alpha^2/2\alpha_0^2}, \tag{19}$$

where α_0 is the variance of α and its second moment is given by $E(\alpha^2) = \overline{\alpha^2} = 2\alpha_0^2$. As $\gamma = \alpha^2 E_0/N_0$ has two real roots, but the Rayleigh distribution does not exist in the negative domain, α_2 can be eliminated and hence $C(\gamma)$ is given by

$$C(\gamma) = \frac{1}{2\alpha_0^2} \frac{N_0}{E_0} \cdot e^{-N_0\gamma/2\alpha_0 E_0}. \tag{20}$$

If we define the average SNR Γ as

$$\Gamma = \bar{\gamma} = E\left\{ \alpha^2 \frac{E_0}{N_0} \right\} = \overline{\alpha^2} \frac{E_0}{N_0} = 2\alpha_0^2 \frac{E_0}{N_0}, \tag{21}$$

where we exploited that $E(\alpha^2) = \overline{\alpha^2} = 2\alpha_0^2$ for a Rayleigh PDF, then the transformed PDF $C(\gamma)$ is given as

$$C(\gamma) = \frac{1}{\Gamma} e^{-\gamma/\Gamma}. \tag{22}$$

This PDF $C(\gamma)$ is known in (22) as the chi-square distribution [13], where the instantaneous SNR $\gamma \geq 0$.

The class I average bit-error probability over Rayleigh-fading channels is found by substituting the PDF $C(\gamma)$ from (22) and the instantaneous bit-error probability $P_{IR}(\gamma)$ over Rayleigh-fading channels from (12), into (14), we get

$$P_{IR}(\Gamma) + \frac{1}{2\Gamma} \int_0^\infty \left[Q\left\{ \sqrt{\frac{\gamma}{5}} \right\} + Q\left\{ 3\sqrt{\frac{\gamma}{5}} \right\} \right] \cdot e^{-\gamma/\Gamma} \, d\gamma. \tag{23}$$

The equations for the CII subchannel cannot be formulated without considering the effect of a particular level of channel attenuation on the demodulation process. The demodulation is now carried out on an attenuated signal constellation. Therefore we multiply the decision boundaries specified in (3) and (4) for the CII bits in the I and Q components by the average attenuation $\bar{\alpha}$ to minimize the number of decision errors. Hence the equations used for the demodulation of the CII I and Q bits are

$$\begin{aligned} &\text{if} \quad I, Q \geq 2\bar{\alpha}d, \quad \text{then} \quad i_2, q_2 = 1 \\ &\text{if} \quad -2\bar{\alpha}d \leq I, Q < 2\bar{\alpha}d, \quad \text{then} \quad i_2, q_2 = 0 \\ &\text{if} \quad -2\bar{\alpha}d > I, Q, \quad \text{then} \quad i_2, q_2 = 1. \end{aligned} \tag{24}$$

Now we focus our attention on the case when the transmitted bit i_2 or q_2 is a logical 0. If i_2 or q_2 having a protection distance d is transmitted, then the modified protection distance between the received phasor $\alpha \cdot d$ and the decision boundary $2\bar{\alpha}d$ is $d_1 = (2\bar{\alpha}d - \alpha d)$. If this modified protection distance is exceeded by a noise sample, an erroneous decision is carried out. By substituting d_1 into (5) instead of d, we get the CII bit-error probability over Rayleigh-fading channels, when a logical 0 was sent as

$$P_{II,R} = Q\left\{ \frac{d_1}{\sqrt{N_0/2}} \right\} = Q\left\{ \frac{d(2\bar{\alpha} - \alpha)}{\sqrt{N_0/2}} \right\}. \tag{25}$$

As the average energy $E_0 = 10d^2$, $d = \sqrt{E_0/10}$, and whence:

$$P_{II,R} = Q\left\{ (2\bar{\alpha} - \alpha)\sqrt{\frac{E_0}{5N_0}} \right\}. \tag{26}$$

From $\gamma = \alpha^2 E_0/N_0$ we get $E_0/N_0 = \gamma/\alpha^2$, and therefore:

$$P_{II,R} = Q\left\{ \left(\frac{2\bar{\alpha} - \alpha}{\alpha} \right)\sqrt{\frac{\gamma}{5}} \right\} = Q\left\{ \left(\frac{2\bar{\alpha}}{\alpha} - 1 \right)\sqrt{\frac{\gamma}{5}} \right\}. \tag{27}$$

The CII bit-error probability for the transmission of a logical 0 can be substituted from (27) along with $C(\gamma)$ from (22) into (14) to give the average CII error probability:

$$\begin{aligned} P_{II,O} &= \int_0^\infty P(\gamma) C(\gamma) \, d\gamma \\ &= \int_0^\infty Q\left\{ \left(\frac{2\bar{\alpha}}{\alpha} - 1 \right)\sqrt{\frac{\gamma}{5}} \right\} \cdot \frac{1}{\Gamma} e^{-\gamma/\Gamma} \, d\gamma. \end{aligned} \tag{28}$$

Let us consider now the reverse situation, when a transmitted CII logical one is corrupted into a logical zero. The modified protection distance is now given by $d_1 = 3\alpha d - 2\bar{\alpha}d$, which is positive, if $3\alpha d > 2\bar{\alpha}d$, i.e., $\alpha/\bar{\alpha} > 2/3$. The AWGN has to overcome this protection distance to cause an error, and hence the CII error probability for a modified protection distance d_1 is

$$P_{II,1} = Q\left\{ \left(\frac{3\bar{\alpha}}{\alpha} - 2 \right)\sqrt{\frac{\gamma}{5}} \right\}. \tag{29}$$

$$P_{II,1}(\Gamma) = \frac{1}{\Gamma} \int_0^\infty Q\left\{ \left(\frac{3\bar{\alpha}}{\alpha} - 2 \right)\sqrt{\frac{\gamma}{5}} \right\} e^{-\gamma/\Gamma} \, d\gamma. \tag{30}$$

For random transmitted data the overall CII subchannel error probability is given by

$$P_{\mathrm{II,R}}(\Gamma) = \frac{1}{2}\left[P_{\mathrm{II,I}}(\Gamma) + P_{\mathrm{II,O}}(\Gamma)\right]. \quad (31)$$

$$P_{\mathrm{II,R}}(\Gamma) = \frac{1}{2\Gamma}\int_0^\infty Q\left\{\left(\frac{2\bar{\alpha}}{\alpha} - 1\right)\sqrt{\frac{\gamma}{5}}\right\} e^{-\gamma/\Gamma}\, d\gamma + \frac{1}{2\Gamma}\int_0^\infty Q\left\{\left(\frac{3\bar{\alpha}}{\alpha} - 2\right)\sqrt{\frac{\gamma}{5}}\right\} e^{-\gamma/\Gamma}\, dy \quad (32)$$

Finally, in case of random transmitted data the average BER over Rayleigh-fading channels is given by

$$P_r = \frac{1}{2}\left[P_{\mathrm{IR}} + P_{\mathrm{IIR}}\right]. \quad (33)$$

References

[1] *Proc. Int. Conf. Digital Land Mobile Radio Commun.*, Venice, June 30,-July 3, 1987.

[2] R. Steele, "Towards a high-capacity digital cellular mobile radio system," *Proc. Inst. Elec. Eng.*, pt. F, vol. 132, no. 5, pp. 405-415, Aug. 1985.

[3] R. Steele and V. K. Prabhu, "High-user density digital cellular mobile radio systems," *Proc. Inst. Elec. Eng.*, pt. F-132, pp. 306-404, Aug. 1985.

[4] K. H. H. Wong and R. Steele, "Transmission of digital speech in highway microcells," *J. Inst. Electron. Radio Eng.*, vol. 57, no. 6, pp. S246-S254, Dec. 1987.

[5] S. T. S. Chia, R. Steele, E. Green, and A. Baran, "Propagation and bit error ratio measurements for a microcellular system," *J. Inst. Electron. Radio Eng.*, vol. 57, no. 6, pp. S255-S266, Dec. 1987.

[6] C.-E. W. Sundberg, W. C. Wong, and R. Steele, "Logarithmic PCM weighted QAM transmission over Gaussian and Rayleigh fading channels," *Proc. Inst. Elec. Eng.*, vol. 134, pt. F, no. 6, pp. 557-570. Oct. 1987.

[7] R. Steele, C.-E. W. Sundberg, and W. C. Wong, "Transmission of log-PCM via QAM over Gaussian and Rayleigh fading channels," *Proc. Inst. Elec. Eng.*, vol. 134, pt. F, no. 6, pp. 539-556, Oct. 1987.

[8] K. H. J. Wong, L. Hanzo, and R. Steele, "A subband codec with embedded Reed-Solomon coding for mobile radio speech communication," *Proc. IEEE Singapore ICCS'88*, pp. 709-713.

[9] L. Hanzo, K. H. H. Wong, and R. Steele, "Efficient channel coding and interleaving schemes for mobile radio communications," in *Proc. Inst. Elec. Eng. Colloquium on Microcellular Mobile Radio*, Feb. 22, 1989, London, Savoy Place.

[10] K. H. H. Wong, L. Hanzo, and R. Steele, "Channel coding for satellite mobile channels," *Int. J. Satellite Commun.*, vol. 7, pp. 143-163, 1989.

[11] W. C. Jakes Ed., *Microwave Mobile Communications*. New York: Wiley, 1974.

[12] K. S. Shanmugam, *Digital and Analog Communication Systems*. New York: Wiley, 1979.

[13] J. G. Proakis, *Digital Communications*. New York: McGraw-Hill, 1983.

[14] R. V. Cox, J. Hagenauer, N. Seshadri, and C. E. Sundberg, "A subband coder designed for combined source and channel coding," in *Proc. ICASSP'88*, pp. 235-238.

[15] R. V. Cox, W. B. Kleijn, and P. Kroon, "Robust CELP coders for noisy backgrounds and noisy channels," *Proc. ICASSP'89*, pp. 739-742.

[16] N. Kitawaki, M. Honda, and K. Itoh, "Speech quality assessment methods for speech coding systems," *IEEE Commun. Mag.*, vol. 22, Oct. 1984.

[17] P. M. Fortune, L. Hanzo, and R. Steele, "Transmission of SBC speech via 16-level QAM over mobile radio channels," in *Proc. GLOBECOM'88*, pp. 832-835.

[18] R. E. Blahut, *Theory and Practice of Error Control Codes*. Reading, MA: Addison-Wesley, 1983.

[19] D. J. Goodman, G. B. Lockhart, O. J. Wasem, and W. C. Wong, "Waveform substitution techniques for recovering missing speech segments in packet voice communications," *IEEE Trans. Acoust., Speech, Signal Processing*, vol. ASSP-34, pp. 1440-1448, Dec. 1986.

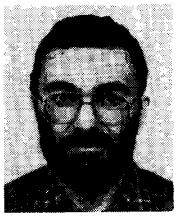

Lajos Hanzo received the M.Sc. and Ph.D. degrees in telecommunications from the Technical University of Budapest, Hungary, in 1976 and 1982, respectively.

From 1976 to 1980 he was involved with research in the field of high-speed data transmission at the Telecommunication Research Institute in Budapest, Hungary. Between 1980 and 1981 he worked at the University of Erlangen-Nürnberg, West Germany. During 1981-1986 his main research interest was speech communication via satellite channels. In 1986 he joined the academic staff of the University of Southampton, England, where he is involved with teaching and researching mobile radio communications. His particular research interests cover source and channel coding, as well as modulation.

Raymond Steele (SM'80) received the B.Sc. degree in electrical engineering from Durham University, Durham, England, in 1959, and the Ph.D. and D. Sc. degrees from Loughborough University of Technology, Loughborough, in 1975 and 1983, respectively.

Prior to attaining the B.Sc. degree, he was an indentured Apprentice Radio Engineer. After research and development posts with E. K. Cole, Cossor Radar and Electronics, and Marconi, he joined the Lecturing Staff at the Royal Naval College, London. He joined Loughborough University in 1968, where he lectured and directed a research group in digital encoding of speech and picture signals. During the summers of 1975, 1977, and 1978 he was a consultant to the Acoustics Research Department at Bell Laboratories, and in 1979 he joined the company's Communications Methods Research Department, Crawford Hill Laboratory, Holmdel, NJ. He returned to England in 1983 to become Professor of Communications in the Department of Electronics and Computer Science at the University of Southampton, a post he retains. From 1983 to 1986 he was a nonexecutive Director of Plessey Research and Technology, and in 1986 he formed Multiple Access Communications, a company concerned with digital mobile radio systems.

Dr. Steele is the author of the book, *Delta Modulation Systems* (New York: Halsted, 1975) and over 100 technical publications. He is Senior Editor of the *IEEE Communications Magazine*. He and his coauthors were awarded the Marconi Premium in 1979 and 1989, and the *Bell System Technical Journal's* Best Mathematics, Communications, Techniques, Computing and Software, and Social Science Paper in 1981.

Peter-Marc Fortune received the B.Sc. and Ph.D. degrees in electronic engineering from the University of Southampton, England, in 1984 and 1988, respectively.

From 1986 to 1988 he worked in communications research at the University of Southampton. Since then he has been studying for the Bachelor of Medicine degree.